Group IVC cytosolic phospholipase $A_2\gamma$ is farnesylated and palmitoylated in mammalian cells

Dawn E. Tucker,* Allison Stewart,* Laxman Nallan,† Pravine Bendale,† Farideh Ghomashchi,† Michael H. Gelb,[1,†] and Christina C. Leslie[1,*,§]

Program in Cell Biology,* Department of Pediatrics, National Jewish Medical and Research Center, Denver, CO 80206; Departments of Chemistry and Biochemistry,† University of Washington, Seattle, WA 98195; and Departments of Pathology and Pharmacology,§ University of Colorado School of Medicine, Denver, CO 80206

Abstract Cytosolic phospholipase $A_2\gamma$ ($cPLA_2\gamma$) is a member of the group IV family of intracellular phospholipase A_2 enzymes, but unlike the well-studied $cPLA_2\alpha$, it is constitutively bound to membrane and is calcium independent. $cPLA_2\gamma$ contains a C-terminal CaaX sequence and is radiolabeled by mevalonic acid when expressed in $cPLA_2\alpha$-deficient immortalized lung fibroblasts ($IMLF^{-/-}$). The radiolabel associated with $cPLA_2\gamma$ was identified as the farnesyl group. The protein farnesyltransferase inhibitor BMS-214662 prevented the incorporation of [^{3}H]mevalonic acid into $cPLA_2\gamma$ and partially suppressed serum-stimulated arachidonic acid release from $IMLF^{-/-}$ and undifferentiated human skeletal muscle (SkMc) cells overexpressing $cPLA_2\gamma$, but not from cells overexpressing $cPLA_2\alpha$. However, BMS-214662 did not alter the amount of $cPLA_2\gamma$ associated with membrane. These results were consistent in COS cells expressing the C538S $cPLA_2\gamma$ prenylation mutant. $cPLA_2\gamma$ also contains a classic myristoylation site and several potential palmitoylation sites and was found to be acylated with oleic and palmitic acids but not myristoylated. Immunofluorescence microscopy revealed that $cPLA_2\gamma$ is associated with mitochondria in $IMLF^{-/-}$, SkMc cells, and COS cells.—Tucker, D. E., A. Stewart, L. Nallan, P. Bendale, F. Ghomashchi, M. H. Gelb, and C. C. Leslie. **Group IVC cytosolic phospholipase $A_2\gamma$ is farnesylated and palmitoylated in mammalian cells. *J. Lipid Res.* 2005.** 46: **2122–2133.**

Supplementary key words prenylation • fatty acylation • mitochondria

Phospholipases A_2 (PLA_2s) hydrolyze the *sn*-2 ester bond of membrane phospholipids and function in the production of lipid mediators, phospholipid acyl-chain remodeling, dietary lipid breakdown, and host defense. Convention divides this family into three main types based on their subcellular localizations and structural differences: the secreted PLA_2s, the intracellular group IV cytosolic phospholipase A_2s ($cPLA_2$s), and the group VI calcium-independent PLA_2s (1). The mammalian secreted PLA_2s constitute a large group of enzymes that have low molecular mass, require calcium for activity, and use a His/Asp dyad in the catalytic mechanism (2, 3). The intracellular PLA_2s, calcium-independent PLA_2s, and $cPLA_2$s have larger molecular masses, use an active site serine, and play a variety of roles in signaling, inflammation, and membrane remodeling, depending on the tissue and cell type (4–9).

One member of the group IV PLA_2 family, group IVA $cPLA_2\alpha$ ($cPLA_2\alpha$), has been well studied because of its specificity for releasing *sn*-2 arachidonic acid from membrane phospholipids for the production of eicosanoids (6, 8, 10). The oxygenated metabolites of arachidonic acid, prostaglandins, and leukotrienes, produced through the cyclooxygenase and lipoxygenase pathways, promote acute inflammatory responses and are also important in regulating many physiological processes (11). $cPLA_2\alpha$ is subject to posttranslational regulatory controls via phosphorylation and Ca^{2+} (12–16). Calcium functions by binding to an N-terminal C2 domain and inducing the translocation of $cPLA_2\alpha$ from the cytosol to the Golgi, endoplasmic reticulum, and nuclear envelope (17–20).

Two additional group IV enzymes have been identified. Group IVC $cPLA_2\gamma$ ($cPLA_2\gamma$) and group IVB $cPLA_2\beta$ ($cPLA_2\beta$); both have ~30% homology to $cPLA_2\alpha$ (21–23). The active site residues found in $cPLA_2\alpha$ are conserved in these paralogs, suggesting that they have a similar catalytic mechanism (22). $cPLA_2\beta$ contains an N-terminal C2 domain that confers calcium sensitivity and an additional N-terminal extension containing a JmjC domain, the function of which is unknown (21–24). In contrast, $cPLA_2\gamma$

Manuscript received 7 June 2005 and in revised form 22 July 2005.

Published, JLR Papers in Press, August 1, 2005.
DOI 10.1194/jlr.M500230-JLR200

Abbreviations: $cPLA_2$, cytosolic phospholipase A_2; GFP, green fluorescent protein; GST, glutathione *S*-transferase; His, 6× histidine tag; IMLF, immortalized mouse lung fibroblasts; PLA_2, phospholipase A_2; Sf9, *Spodoptera frugiperda*; SH, sulfhydryl; SkMc, skeletal muscle.

[1] To whom correspondence should be addressed.
e-mail: gelb@chem.washington.edu (M.H.G.);
lesliec@njc.org (C.C.L.)

does not contain a C2 domain, consistent with its lack of regulation by Ca^{2+} (21, 22). The regulatory phosphorylation sites used by cPLA$_2\alpha$ are not present in cPLA$_2\gamma$, although it possesses multiple putative PKC phosphorylation sites, the use of which has yet to be investigated. Unlike cPLA$_2\alpha$ and cPLA$_2\beta$, which are widely distributed in mammalian tissues, cPLA$_2\gamma$ message is abundantly expressed in skeletal muscle (SkMc), brain, and heart (21, 22). In another significant departure from cPLA$_2\alpha$, cPLA$_2\gamma$ and cPLA$_2\beta$ do not exhibit strong *sn*-2 acyl chain specificity (25, 26). cPLA$_2\gamma$ exhibits relatively high lysophospholipase activity, as reported previously for cPLA$_2\alpha$ (25, 27).

A unique property of cPLA$_2\gamma$ is that it is constitutively bound to cell membrane and contains putative acylation sites and a C-terminal prenylation site that may regulate its membrane association (21). The C-terminal sequence CCLA on cPLA$_2\gamma$ fits the consensus sequence of a CaaX box (a is usually, but not necessarily, an aliphatic residue), a motif that is recognized by protein prenyltransferases for the attachment of either a 15 carbon farnesyl or a 20 carbon geranylgeranyl to the cysteine sulfhydryl (SH) group (28, 29). Indeed, cPLA$_2\gamma$ becomes radiolabeled when expressed in COS cells grown in the presence of [^{3}H]mevalonic acid, the precursor of prenyl groups in mammalian cells (21). The structure of the prenylated C terminus cannot be inferred from the cPLA$_2\gamma$ CaaX sequence. The CCLA sequence could be recognized by protein farnesyltransferase, resulting in the attachment of a farnesyl group to the N-terminal-most cysteine SH.

cPLA$_2\gamma$ has been shown to be farnesylated when expressed in insect cells (30); however, the structure of the prenyl group on cPLA$_2\gamma$ in mammalian cells has not been investigated. cPLA$_2\gamma$ could also be a substrate for protein geranylgeranyltransferase type I, resulting in geranylgeranylation of the N-terminal-most cysteine SH. Finally, it may be noted that a subset of Rab GTPases contain the C-terminal sequence CCXX, and the enzyme protein geranylgeranyltransferase type II attaches a geranylgeranyl group to each of the two cysteine SH groups (31). Thus, cPLA$_2\gamma$ could be a doubly geranylgeranylated protein in mammalian cells. cPLA$_2\gamma$ also contains a putative myristoylation site as well as several potential fatty acylation sites.

Both myristoylation and palmitoylation are widespread fatty acid modifications on membrane-associated proteins. In addition to facilitating high-affinity membrane association on dually lipidated proteins, these modifications can aid in protein trafficking of enzymes to specific compartments or subdomains (32, 33). Palmitoylation has also been implicated in the regulation of enzymatic activity in proteins, notably multiple mitochondrial enzymes (34–36). In the present study, we have found that cPLA$_2\gamma$ is farnesylated and acylated in mammalian cells. Prenylation of cPLA$_2\gamma$ was also found to be important for the function of cPLA$_2\gamma$ in intact cells. In addition, we have found that cPLA$_2\gamma$ is localized to the mitochondria when expressed in mammalian cells.

METHODS

Materials

The protein farnesyltransferase inhibitor BMS-214662 was prepared as described (37). An analog of BMS-214662 containing a methyl group at N1 of the imidazol ring (Me-BMS-214662) was prepared similarly. The compounds were purified by HPLC on a C18 reverse-phase column and shown to have the correct structure by ^{1}H-NMR and electrospray ionization mass spectrometry. Simvastatin lactone (a gift from Merck, Rahway, NJ) was saponified by dissolving 25.5 mg in 520 μl of 0.1 M NaOH, adding an equal volume of 150 mM NaCl, and incubating at 60°C for 3 h until the simvastatin was dissolved. The pH was adjusted to 7.0 with 0.1 N HCl, and the solution was filter-sterilized and stored at −20°C. [5,6,8,9,11,12,14,15-^{3}H]arachidonic acid (specific activity, 100 Ci/mmol), [^{3}H]mevalonic acid (specific activity, 40 Ci/mmol), [^{3}H]palmitic acid (specific activity, 45 Ci/mmol), and [^{3}H]myristic acid (specific activity, 60 Ci/mmol) were from Perkin-Elmer Life Sciences. Amplify, used for fluorography of tritiated bands on polyacrylamide gels, was from Amersham. Mouse serum was from Atlanta Biologicals. Clonetics™ SkMc cells and growth media were from Cambrex (Rutherford, NJ). HEK293 (QBI-293A) cells and adenovirus containing the gene for green fluorescent protein (GFP) were obtained from Qbiogene (Carlsbad, CA). Production of baculovirus and adenovirus for expression of cPLA$_2\gamma$ in *Spodoptera frugiperda* (Sf9) and mammalian cells, respectively, was carried out as described previously (25). The mitochondrion-specific monoclonal antibody to oxidative phosphorylation complex V, subunit b, and the secondary antibodies used for immunofluorescence were from Molecular Probes.

cPLA$_2\gamma$ polyclonal antibody production and Western blot analysis

Human cPLA$_2\gamma$ was cloned as described previously (25). To produce glutathione *S*-transferase (GST)-cPLA$_2\gamma$, cPLA$_2\gamma$ was cloned into the *Eco*RI/*Pst*I sites of pAcGHLT baculovirus transfer vector, and baculovirus was generated as described previously (25). Sf9 cells grown in suspension (500 ml) were infected with baculovirus for 48 h and lysed in 50 mM Hepes buffer, pH 7.4, 150 mM NaCl, 10% glycerol, 1% Triton X-100, 1 mM EGTA, 1 mM EDTA, and one complete protease inhibitor cocktail tablet per 50 ml (Roche). GST-cPLA$_2\gamma$ was affinity-purified using glutathione agarose beads by standard protocols. GST-cPLA$_2\gamma$ (50–100 μg) was added to an equal volume of complete Freund's adjuvant and injected subcutaneously into rabbits. Subsequent booster injections were carried out every 3 weeks using Freund's incomplete adjuvant. Antiserum was obtained 10 days after each injection and analyzed for reactivity to cPLA$_2\gamma$ by Western blotting.

Cell homogenates for Western blot analysis of cytosol and membrane fractions were prepared by sonicating cells in 50 mM Hepes, pH 7.4, containing 0.34 M sucrose, 1 mM EGTA, 10% glycerol, 10 μg/ml leupeptin, 10 μg/ml aprotinin, and 1 mM phenylmethylsulfonyl fluoride. Homogenates were centrifuged at 100,000 *g* for 45 min to obtain the cytosol and membrane fractions. The protein concentration of the cell fractions was determined using the bicinchoninic acid reagent. Lysates were diluted in Laemmli buffer, and proteins were separated on 10% polyacrylamide gels, transferred to nitrocellulose, and blocked for 1 h in Tris-buffered saline containing 0.25% Tween 20 and 5% nonfat dry milk. Nitrocellulose membranes were incubated overnight in a 1:1,000 dilution of anti-cPLA$_2\gamma$ antiserum, and immunoreactive protein was detected using the Amersham Biosciences ECL system.

Cell culture, production of DNA constructs, and recombinant adenovirus

Immortalized mouse lung fibroblasts lacking group IVA cPLA$_2\alpha$ (IMLF$^{-/-}$) were isolated and immortalized with SV40, as described previously (38). The replication-deficient recombinant adenoviruses carrying the cDNA for untagged cPLA$_2\gamma$ (Ad-cPLA$_2\gamma$) and for GFP-tagged cPLA$_2\alpha$ (Ad-GFPcPLA$_2\alpha$) were generated using the AdEasy vector system (Qbiogene) and titered, and expression levels were determined as described previously (25). Freshly isolated human SkMc cells obtained from Cambrex were grown in complete human SkMc growth medium for two passages and then frozen. Cells were thawed and passaged once by trypsinization according to the manufacturer's protocol (Cambrex) before use in experiments. The C538 in the CaaX box of cPLA$_2\gamma$ was mutated to a serine (C538S) using PCR-based site-directed mutagenesis (Stratagene) and the primer 5′-CTA TGC CAA GCA GCT ACT TCG GGC ACT-3′. The putative N-myristoylation site (G2) was mutated to alanine (G2A) by the same method. The primer used was 5′-TTC GGA CCG CAG TGC ACC ATG GCA AGC TCT GAA GTT-3′. The C-terminal truncated cPLA$_2\gamma$ was created by mutating K490 into a TAG stop codon using the primer 5′-GAC ACA TAC GAC ACA TTC TAG CTT GCT GAC-3′. Wild-type and mutant cPLA$_2\gamma$ were cloned into the pcDNA3.0 mammalian expression vector. All constructs were confirmed by sequencing. COS and HEK293 cells were transiently transfected using FuGENE transfection reagent according to the manufacturer's instructions (Roche Diagnostics, Indianapolis, IN). Expression of wild-type and mutant cPLA$_2\gamma$ was confirmed by Western blotting. RT-PCR of endogenous cPLA$_2\gamma$ in SkMc cells was conducted using 5′-GCT CAC ATT GCC TGC CTT GGG GTC CTG-3′ and 5′-AGT GCC CGA AGT TGC TGC TTG GCA TAG-3′ and RNA isolated with the RNeasy mini kit (Qiagen).

Structural analysis of the cPLA$_2\gamma$ prenyl group

IMLF$^{-/-}$ were plated at 1×10^6 cells/100 mm dish and incubated for 10 h in DMEM containing 2% FBS. The cells were washed and incubated in 4 ml of serum-free DMEM containing 0.1% BSA and Ad-cPLA$_2\gamma$ as described previously (25). After incubation for 90 min, additional DMEM containing 0.1% BSA, 1 mCi of [^{3}H]mevalonic acid, and 10 μM simvastatin was added to the cells to prevent the mevalonate from becoming metabolized to cholesterol. For some experiments, the medium also included 1 μM of the farnesyltransferase inhibitor BMS-214662 or Me-BMS-214662. After incubation for 26 h, cells were rinsed with PBS and solubilized in ice-cold lysis buffer (50 mM Hepes, pH 7.4, 150 mM sodium chloride, 1% Nonidet P-40, 200 μM sodium orthovanadate, 10 mM tetrasodium pyrophosphate, 100 mM sodium fluoride, 10 μg/ml leupeptin, 10 μg/ml aprotinin, 100 μM phenylmethylsulfonyl fluoride, and 300 nM *p*-nitrophenyl phosphate). The lysate was incubated at 0°C for 15 min, then centrifuged for 10 min at 4°C at full speed in a microfuge. Total protein in the supernatant was quantified using the bicinchoninic acid method. Immunoprecipitation of cPLA$_2\gamma$ was carried out by incubating the lysates at 4°C with protein A-Sepharose beads and anti-cPLA$_2\gamma$ antiserum (1:25) overnight while rotating. The beads were washed five times in lysis buffer and then boiled in Laemmli buffer for 10 min. One-third of the labeled proteins was separated by SDS-PAGE, and the gel was fixed in isopropanol-water-acetic acid (25:65:10) for 10 min. The gel was incubated for 30 min in Amplify at room temperature before drying and then exposed to film for 8 days for visualization of the bands.

For samples to be extracted for HPLC prenylation analysis, the remaining two-thirds of the immunoprecipitate was electrophoresed and dried without fixation or Amplify treatment. The pieces of dried gel corresponding to the location of radiolabeled cPLA$_2\gamma$ (61 kDa) were excised. Protein in the gel slices was extracted in the presence of 100 mg of BSA as carrier (39), and half of the extract was further processed. Extracted protein was precipitated with trichloroacetic acid, and the precipitate was washed with cold acetone as described (39). The dried protein was dissolved in guanidine-HCl/sodium phosphate buffer, *N*-acetyl-cysteine(*S*-farnesyl) and *N*-acetyl-cysteine(*S*-geranylgeranyl) (20 mg each; Bachem, Inc.) were added, and the sample was treated with Raney-nickel as described (39). The pentane extract was concentrated and submitted to HPLC analysis, and radioactivity in the column fractions was determined by scintillation counting (39).

Analysis of cPLA$_2\gamma$ fatty acylation

Adenoviral infection and immunoprecipitation were modified from the protocol for the farnesylation experiments described above. IMLF$^{-/-}$ cells were cultured in serum-free DMEM containing 0.1% fatty acid-free BSA for 22 h and then incubated for 4 h in the same medium containing either 0.3 mCi/ml [^{3}H]palmitate or 0.1 mCi/ml [^{3}H]myristate. After immunoprecipitation of cPLA$_2\gamma$ (as described above), proteins were separated by SDS-PAGE and the gels were either submitted to fluorography or incubated briefly in water and dried. For analysis of fatty acylation, bands corresponding to cPLA$_2\gamma$ were excised. The gel slice was mixed in 1 ml of 50% aqueous methanol at room temperature in a polypropylene tube. After 2–3 h, the liquid was removed and the gel slice was washed again as above. The gel slice was dried with a Speed-Vac (Savant Instruments), and 0.7 ml of 1.5 M aqueous NaOH was added to the tube. After incubation for 2 h at 30°C, the solution was brought to pH ~2 by the addition of 6 M HCl (monitored with pH paper). The gel slice and solution were transferred to a glass tube, and 2.5 ml of Dole solvent (24 ml of isopropanol, 0.6 ml of 0.5 M H_2SO_4, and 6 ml of *n*-heptane) was added (using a portion to rinse the polypropylene tube). The sample was vortexed, 1 ml of water and 1.5 ml of *n*-heptane were added, and the sample was vortexed again.

The upper organic phase was transferred to a glass tube, and solvent was removed from the organic and aqueous phases with a Speed-Vac. To the tube containing the residue from the aqueous phase and gel slice was added 0.7 ml of 6 M HCl, the top of the tube was sealed with a glassblower torch, and the tube was heated in an incubator for 4 h at 100°C. After cooling, the tube was opened with the aid of a scoring file, and solvent was removed with a Speed-Vac. Water was added to the residue (0.7 ml), and the sample was extracted by the addition of Dole solvent, water, and *n*-heptane as described above. The upper organic phase was transferred to a glass tube, and the solvent was removed from both tubes with a Speed-Vac. Methanol (1 ml) was added to each tube, and the radioactivity in 0.1 ml aliquots was determined by scintillation counting.

Methanol in the tube containing the organic extract of the NaOH-treated and HCl-acidified sample (see above) was transferred to a 1.5 ml vial with a Teflon-septum screw cap, 1 mmol each of myristic acid, palmitic acid, and oleic acid were added (from 50 mM stock solutions in methanol), and solvent was removed with a Speed-Vac. Diisopropylethylamine (0.5 ml of 10%, v/v; Aldrich) and 1% (v/v) pentafluorobenzyl bromide (Pierce) in CH_3CN was added to the residue, and the capped vial was heated at 60°C for 15 min. An overnight Speed-Vac treatment removed the solvent and excess reagents. The residue was dissolved in CH_3CN and injected onto a C18 reverse-phase HPLC column (1 × 25 cm; Vydac 218TP1010) equilibrated previously with 70% CH_3CN in water at a flow rate of 1.5 ml/min. The column was developed with a solvent gradient of 70% CH_3CN in wa-

ter to 100% CH_3CN over 20 min and then held at 100% CH_3CN for 60 min. Absorbance at 254 nm was monitored, and 2 min fractions were collected into scintillation vials. Solvent was removed with a Speed-Vac, and the residues were dissolved in scintillation fluid and counted.

Arachidonic acid release assays

Cells were plated at 1.25×10^4 cells/cm^2 on 24-well plates in DMEM containing 2% FBS for IMLF$^{-/-}$ or in complete SkMc medium for growing SkMc cells and incubated overnight. COS cells were plated at the same density and transfected as described above. The cells were washed and then incubated in 150 μl of DMEM containing 0.1% BSA with Ad-cPLA$_2\gamma$ or Ad-GFP control virus. After incubation for 90 min, DMEM (500 μl) containing 0.1% BSA and 0.2 μCi/ml [^{3}H]arachidonic acid was added. In some experiments 1 μM BMS-214662 or Me-BMS-214662 was added. After a 26 h incubation, cells were washed two times in medium containing 0.1% BSA to remove unincorporated arachidonic acid. Cells in this medium were then stimulated with 10% mouse serum for 3 h (25). The amount of radioactivity released into the medium was determined and expressed as a percentage of the total counts incorporated into the cells.

Immunofluorescence microscopy

IMLF$^{-/-}$ or SkMc cells were plated on 35 mm glass-bottomed MatTek plates at 1.25×10^4 cells/cm^2 and infected with Ad-cPLA$_2\gamma$ as described above. The cells were rinsed once with PBS and incubated for 15 min in ice-cold fixative containing 3.2% paraformaldehyde and 3% sucrose in PBS. After fixation, cells were rinsed five times with cold PBS and incubated for 15 min in 0.1% Triton X-100 in PBS. Cells were then rinsed with PBS and blocked for 1 h in PBS containing 10% FBS. Fixed cells were incubated with anti-cPLA$_2\gamma$ polyclonal antiserum (1:50) overnight, followed by a 2 h incubation with goat anti-rabbit Texas Red-conjugated secondary antibody (1:100). Cells were costained with mitochondrion-specific anti-oxidative phosphorylation complex V monoclonal antibody (1:20) and an AlexaFluor 488-conjugated anti-mouse secondary antibody (1:100). Control experiments with Texas Red anti-rabbit secondary antibody only and with both primary antibodies and both secondary antibodies were included to identify any nonspecific reactions. After incubation with each antibody, the cells were washed five times in PBS containing 10% FBS. All antibodies were diluted into blocking solution and centrifuged at full speed in a microfuge before use. Controls using secondary antibodies alone were included and revealed only a low level of background fluorescence (data not shown). IMLF$^{-/-}$ were visualized using a Nikon diaphot inverted microscope with a 60×, 1.4 numerical aperture oil-immersion lens and a Photometrics charge-coupled device camera using FITC and Tetramethyl Rhodamine Iso-Thiocyanate filters. Images were acquired with IP Labs software (Scanalytics, Inc.). Immunofluorescence microscopy of SkMc cells was carried out using an Olympus inverted microscope with a 60×, 1.25 numerical aperture oil-immersion objective, and images were collected with a charge-coupled device camera using Chroma dichroic mirrors fitted with emission filters for FITC and Texas Red detection. Image acquisition and analysis were performed using TILL visION software (TILL Photonics).

RESULTS

cPLA$_2\gamma$ is farnesylated in mammalian cells

IMLF$^{-/-}$ infected with Ad-cPLA$_2\gamma$ were grown in the presence of [^{3}H]mevalonic acid followed by immunoprecipitation of cPLA$_2\gamma$. One-third of the total volume of the immunoprecipitate was resolved by SDS-PAGE, and the gel was submitted to fluorography. As shown in **Fig. 1A**, a major radioactive band was seen with an apparent molecular mass of ~60 kDa, which is the predicted molecular mass of cPLA$_2\gamma$, demonstrating that cPLA$_2\gamma$ is labeled by mevalonic acid, consistent with previous results (21). The remaining two-thirds of the immunoprecipitate was resolved by SDS-PAGE but not submitted to fluorography, and a gel piece corresponding to the cPLA$_2\gamma$ region was excised. Protein was eluted from the gel slice and treated with Raney-nickel, which cleaves the carbon-sulfur bond of protein prenyl groups (31, 39). HPLC analysis of the released radiolabeled material clearly shows that it comigrates with the 15 carbon trimethyl dodecatriene (fraction 32) and that no 20 carbon material was detected (Fig. 1B). The results demonstrate that cPLA$_2\gamma$ is a farnesylated protein in mammalian cells.

Functional effects of farnesylation inhibition

The tetrahydrobenzodiazepine analog BMS-214662 is a potent inhibitor of mammalian protein farnesyltransferase, with an IC_{50} of 1.35 nM (37). BMS-214662 is also cell-permeable, as 100 nM causes 60% reversion of the transformation of Rat-1 fibroblasts that express oncogenic Ras GTPase (37). Thus, we tested BMS-214662 for its ability to block the incorporation of [^{3}H]mevalonic acid into cPLA$_2\gamma$ expressed in IMLF$^{-/-}$. cPLA$_2\gamma$ was immunopre-

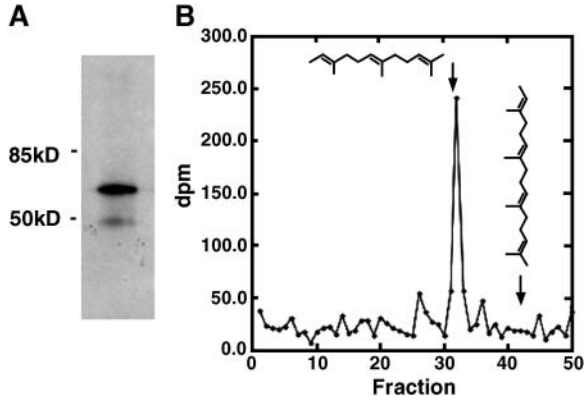

Fig. 1. Cytosolic phospholipase A$_2\gamma$ (cPLA$_2\gamma$) is farnesylated when expressed in immortalized mouse lung fibroblasts lacking group IVA cPLA$_2\alpha$ (IMLF$^{-/-}$). A: cPLA$_2\gamma$ was immunoprecipitated from [^{3}H]mevalonic acid-labeled IMLF$^{-/-}$, separated by SDS-PAGE, and subjected to fluorography. B: Reverse-phase HPLC analysis of the radiolabeled hydrocarbon material released from immunoprecipitated cPLA$_2\gamma$ that was treated with Raney-nickel. Fractions were collected every 2 min and submitted to scintillation counting to provide dpm of radioactive material, which is plotted. The arrows indicate the elution positions of the 15 carbon all-*trans*-2,6,10-trimethyl-2,6,10-dodecatriene (derived from the farnesyl group) and the 20 carbon all-*trans*-2,6,10,14-tetramethyl-2,6,10,14-hexadecateratraene (derived from the geranylgeranyl group). These retention times are derived by monitoring the absorbance at 210 nm (not shown) to detect the authentic hydrocarbons derived from Raney-nickel cleavage of the *N*-acetyl-cysteine(*S*-prenyl) standards that were added to the reaction mixture (see Methods).

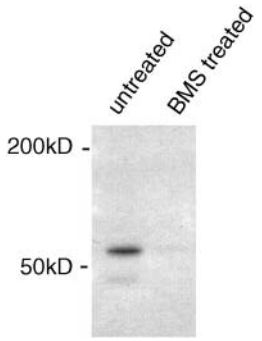

Fig. 2. Inhibition of [^{3}H]mevalonic acid labeling of cPLA$_2\gamma$ with the protein farnesyltransferase inhibitor BMS-214662. IMLF$^{-/-}$ were infected with Ad-cPLA$_2\gamma$ and incubated with or without 1 μM BMS-214662. cPLA$_2\gamma$ was immunoprecipitated, separated by SDS-PAGE, and subjected to fluorography.

cipitated from both untreated cells and cells exposed to 1 μM BMS-214662. A radiolabeled band at ~60 kDa was present in untreated cells. As shown in **Fig. 2**, incorporation of [^{3}H]mevalonic acid into the 60 kDa cPLA$_2\gamma$ band was almost completely blocked by the farnesyltransferase inhibitor BMS-214662. The inhibitor was added to the cells at the time of adenovirus infection to prevent the prenylation of cPLA$_2\gamma$ as it was being expressed. Prenylation is thought to be an irreversible modification; therefore, the inhibitor would not cause the loss of the prenyl group from an existing pool of cPLA$_2\gamma$ protein. BMS-214662 did not affect the levels of cPLA$_2\gamma$ expression (see Fig. 5).

To analyze the potential role of prenylation on cPLA$_2\gamma$ function, the effect of BMS-214662 on [^{3}H]arachidonic acid release from IMLF$^{-/-}$ expressing cPLA$_2\gamma$ was determined. We have previously reported that cPLA$_2\gamma$ expressed in IMLF$^{-/-}$ is activated by serum, resulting in the release of arachidonic acid and other fatty acids (25). IMLF$^{-/-}$ were infected with Ad-cPLA$_2\gamma$, and with Ad-GFP as a control, and the effect of BMS-214662 on serum-induced arachidonic acid release was determined. As shown in **Fig. 3** (upper panel), there was increased arachidonic acid release from IMLF$^{-/-}$ expressing cPLA$_2\gamma$ compared with control cells infected with Ad-GFP, and BMS-214662 inhibited cPLA$_2\gamma$-mediated [^{3}H]arachidonic acid release by ~60%. A recent study has shown that mutation of the CaaX sequence also suppresses A23187-stimulated arachidonic acid release in HEK293 cells overexpressing cPLA$_2\gamma$ (40).

To determine the specificity of the inhibitor, the effect of BMS-214662 on cPLA$_2\alpha$-mediated arachidonic acid release was tested (Fig. 3, lower panel). Serum stimulation of IMLF$^{-/-}$ expressing cPLA$_2\alpha$ resulted in a large increase in arachidonic acid release compared with control cells, as we reported previously, and this response was unaffected by the protein farnesyltransferase inhibitor. Similar experiments were carried out in primary cultures of SkMc cells to determine whether prenylation of cPLA$_2\gamma$ plays a functional role (**Fig. 4**). SkMc cells overexpressing cPLA$_2\gamma$ released more arachidonic acid in response to mouse serum

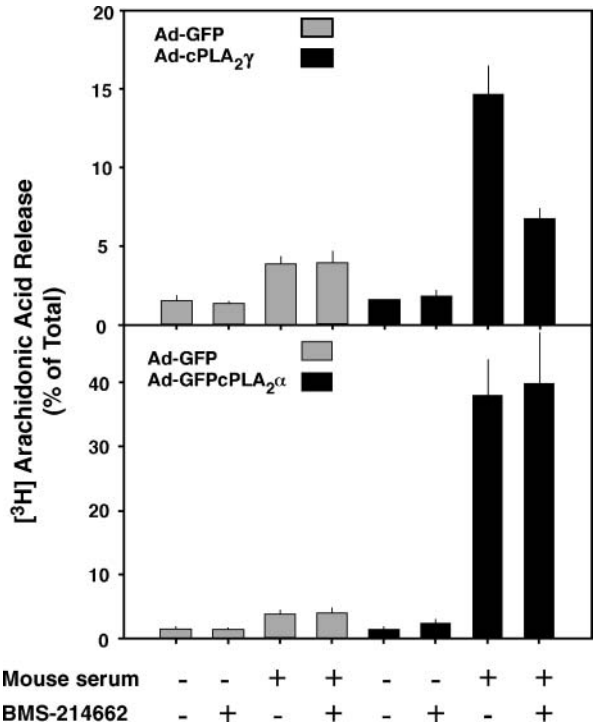

Fig. 3. BMS-214662 inhibits cPLA$_2\gamma$-mediated arachidonic acid release from IMLF$^{-/-}$. IMLF$^{-/-}$ were infected with Ad-cPLA$_2\gamma$ and Ad-green fluorescent protein (GFP) control virus (upper panel) or Ad-GFPcPLA$_2\alpha$ and Ad-GFP control virus (lower panel) and incubated with or without 1 μM BMS-214662 in medium containing [^{3}H]arachidonic acid. The cells were washed and then stimulated with 10% mouse serum for 3 h. The amount of radioactivity released into the medium is expressed as a percentage of the total incorporated radioactivity. Data shown are the average ±SEM of three independent experiments.

than control cells infected with Ad-GFP, and cPLA$_2\gamma$-mediated arachidonic acid release was inhibited to near basal levels by BMS-214662. Another inhibitor, Me-BMS-214662, which inhibits mammalian protein farnesyltransferase with a similar potency as BMS-214662 (M. Gelb, unpublished observation), similarly suppressed arachidonic acid release from SkMc cells expressing cPLA$_2\gamma$. Arachidonic acid release experiments were also conducted using transiently transfected COS cells overexpressing both the wild type and the cPLA$_2\gamma$ C538S prenylation mutant. Consistent with the inhibitor experiments, the mutation partially prevented arachidonic acid release by cPLA$_2\gamma$ in COS cells (Fig. 4B).

Effect of prenylation on membrane association of cPLA$_2\gamma$

To determine whether the farnesylation of cPLA$_2\gamma$ is necessary for its constitutive association with membrane, the effects of BMS-214662 and the C538S prenylation mutant on the relative amounts of cPLA$_2\gamma$ in the cytosol and on the membrane were investigated. IMLF$^{-/-}$ and SkMc cells were infected with Ad-cPLA$_2\gamma$ in the presence and absence of 1 μM BMS-214662, and the relative levels of cPLA$_2\gamma$ in the 100,000 *g* soluble and particulate fractions were determined by Western blotting. Infection of both cell types with Ad-cPLA$_2\gamma$ resulted in increased levels of

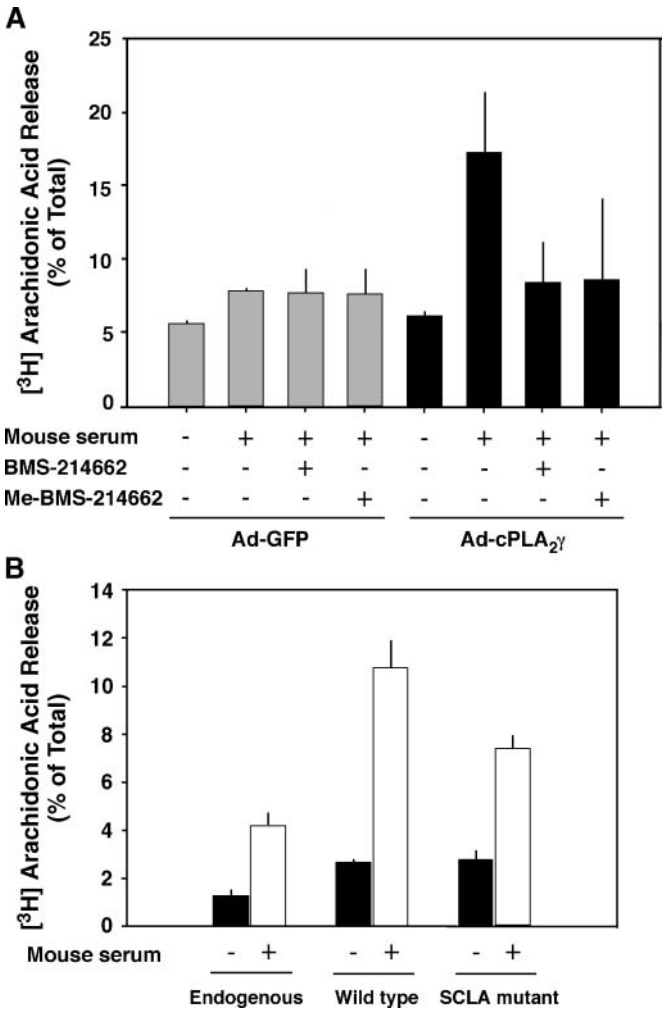

Fig. 4. A: Protein farnesyltransferase inhibitors suppress serum-stimulated arachidonic acid release from skeletal muscle (SkMc) cells overexpressing cPLA$_2\gamma$. SkMc cells were infected with Ad-cPLA$_2\gamma$ and Ad-GFP control virus and incubated with or without 1 μM BMS-214662 or Me-BMS-214662 in medium containing [^{3}H]arachidonic acid. The cells were washed and then stimulated with 10% mouse serum for 3 h. The amount of radioactivity released into the medium is expressed as a percentage of the total incorporated radioactivity. B: Inhibition of farnesylation of cPLA$_2\gamma$ by mutating the C-terminal CaaX box cysteine to a serine reduces fatty acid release by cPLA$_2\gamma$ in transiently transfected COS cells. COS cells were transiently transfected with both wild-type and mutant cPLA$_2\gamma$ using FuGENE transfection reagent. Expression of cPLA$_2\gamma$ protein was confirmed by Western blotting (data not shown). Data shown are averages ± SEM of three independent experiments.

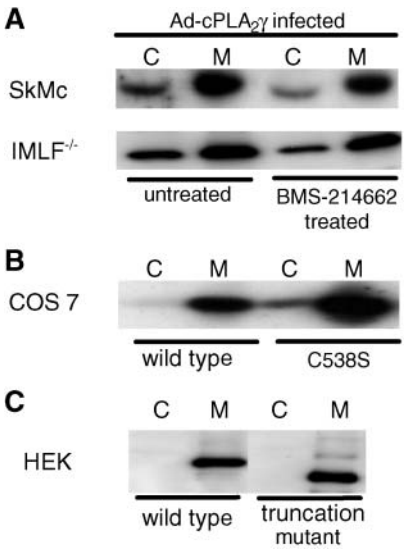

Fig. 5. Membrane association of cPLA$_2\gamma$ is not determined by the C-terminal region or farnesylation. A: Cell homogenates of IMLF$^{-/-}$ and SkMc cells infected with Ad-cPLA$_2\gamma$ and incubated with or without BMS-214662 were prepared as described in Methods. The relative amount of cPLA$_2\gamma$ in the 100,000 *g* soluble (cytosol; C) and particulate (membrane; M) fractions was determined by Western blot analysis of 30 μg of total protein per lane. B: Cell homogenates of COS cells overexpressing cPLA$_2\gamma$ with the C-terminal CaaX sequence mutated were prepared as described in Methods. Amounts of mutated cPLA$_2\gamma$ in the soluble (C) and particulate (M) fractions were determined by Western blotting. C: Cell homogenates of HEK cells overexpressing an ~55 kDa cPLA$_2\gamma$ with the C terminus truncated were prepared as described in Methods. Amounts of mutated cPLA$_2\gamma$ in the soluble (C) and particulate (M) fractions were determined by Western blotting.

cPLA$_2\gamma$ that were predominantly associated with the membrane, although a lower level was observed in the soluble fraction, as reported previously in CHO and Sf9 cells overexpressing cPLA$_2\gamma$ (**Fig. 5**) (21, 25). Inhibition of prenylation, by treatment of the cells with BMS-214662 (Fig. 5A) or expression of the C538S prenylation mutant (Fig. 5B), had no effect on the distribution of cPLA$_2\gamma$, which remained primarily membrane-associated. This is consistent with previous findings showing that mutation of the CaaX sequence and the putative myristoylation site does not affect the membrane binding of cPLA$_2\gamma$ expressed in CHO cells (21). In contrast, a recent study has suggested that mutation of the CaaX sequence partially decreases the affinity of cPLA$_2\gamma$ for membrane in HEK293 cells based on enzymatic assays, although the relative amount of cPLA$_2\gamma$ present in the membrane by Western blot analysis was not determined (40). In our experiments, transfection of C538S mutant cPLA$_2\gamma$ into HEK293 cells did not result in a change in membrane distribution of the cPLA$_2\gamma$ according to Western blotting (data not shown). In addition, when membranes (100,000 *g* pellet) from COS cells expressing cPLA$_2\gamma$ mutated at the prenylation site (C538S) were treated with 1.0 M NaCl, cPLA$_2\gamma$ remained associated with the membrane (data not shown).

To determine whether the hydrophobic and basic regions in the C terminus of cPLA$_2\gamma$ play a role in the membrane association of the enzyme, the C terminus of cPLA$_2\gamma$ was truncated. The addition of a stop codon replacing a lysine (K490) allowed the expression of an ~55 kDa truncated version of cPLA$_2\gamma$. The truncation also removed the CaaX sequence, thus preventing farnesylation of the enzyme, in addition to removing the hydrophobic and basic regions of the enzyme. Overexpression of the truncated cPLA$_2\gamma$ and separation of the membrane fraction (100,000 *g*) in HEK293 cells indicated that without these regions, cPLA$_2\gamma$ remained associated with the membrane (Fig. 5C).

Fatty acylation of cPLA$_2\gamma$

IMLF$^{-/-}$ infected with Ad-cPLA$_2\gamma$ were incubated in medium containing [^{3}H]palmitate or [^{3}H]myristate for 4 h, followed by immunoprecipitation of cPLA$_2\gamma$, separation by SDS-PAGE, and fluorography to visualize tritiated bands. As shown in **Fig. 6A**, major radioactive bands were seen with an apparent molecular mass of ~60 kDa, the predicted molecular mass of cPLA$_2\gamma$, demonstrating that cPLA$_2\gamma$ is labeled by [^{3}H]fatty acids. Samples from separate experiments were treated identically but not submitted to fluorography, and a gel piece corresponding to the cPLA$_2\gamma$ region was excised. When the gel slice containing immunoprecipitated cPLA$_2\gamma$ obtained from [^{3}H]myristate- or [^{3}H]palmitate-labeled cells was washed three times with 50% aqueous methanol, <1% of the total radioactivity in the gel slice was obtained in the combined washes. This shows that all of the radiolabel is protein bound (i.e., that there are no free radiolabeled fatty acids in the gel slice).

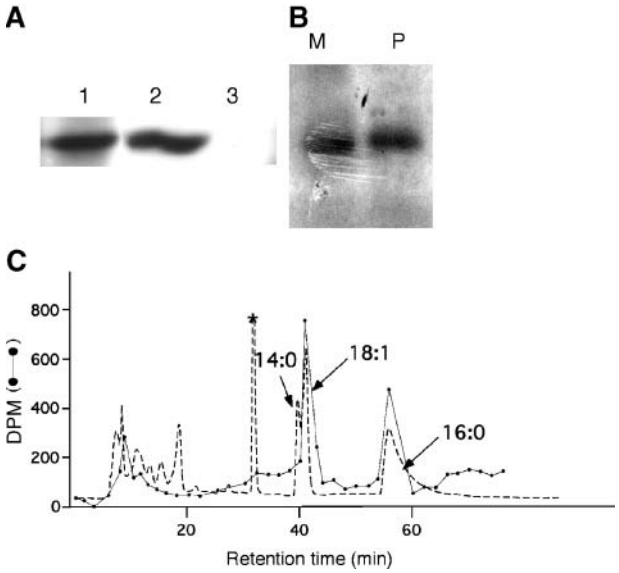

Fig. 6. cPLA$_2\gamma$ is acylated with palmitic and oleic acids but it is not myristoylated. A: cPLA$_2\gamma$ was immunoprecipitated from cell homogenates of IMLF$^{-/-}$ cells infected with Ad-cPLA$_2\gamma$ using anti-cPLA$_2\gamma$ antiserum (lane 1) or preimmune serum (lane 3) and analyzed by Western blotting using anti-cPLA$_2\gamma$ antiserum. The Western blot of homogenate, before immunoprecipitation, is shown in lane 2. B: cPLA$_2\gamma$ was immunoprecipitated from [^{3}H]palmitic (P) or [^{3}H]myristic (M) acid-labeled IMLF$^{-/-}$, separated by SDS-PAGE, and subjected to fluorography. C: HPLC analysis of fatty acid esters released from cPLA$_2\gamma$. Fatty acids released from cPLA$_2\gamma$ by treatment with aqueous NaOH were converted to their pentafluorobenzyl esters. The dashed line represents the absorbance at 254 nm and reveals the position of the pentafluorobenzyl esters of the nonradiolabeled fatty acid standards added to the reaction mixture: myristic acid (14:0), oleic acid (18:1), and palmitic acid (16:0) (indicated by arrows). The absorbance peak marked with an asterisk is derived from esterification reagents, because it was seen in a blank run containing only reagents. The absorbance peaks eluting earlier than 20 min are attributable to unknown substances, presumably hydrophilic material derived from impurities present in the cPLA$_2\gamma$ sample. The dotted line indicates the amount of tritium (dpm) in each column fraction. The total dpm of tritium eluting from the column is 85% of that injected.

The washed gel slice was treated with 1.5 M aqueous NaOH at 30°C for 2 h, conditions known to hydrolyze thiolester- or oxyester-linked fatty acid groups from proteins (41). It was found that 35% and 38% of the total radioactivity in the gel slice was obtained in the organic phase of the Dole solvent extract from [^{3}H]myristate- and [^{3}H]palmitate-labeled cells, respectively.

When the remaining gel slice and residue in the water layer was hydrolyzed in 6 M HCl at 100°C for 4 h, conditions that lead to the hydrolysis of amide-linked fatty acyl groups, 8% and 6% of the total gel slice radioactivity was recovered in the Dole solvent extract from [^{3}H]myristate- and [^{3}H]palmitate-labeled cells, respectively. Fifty-seven percent and 56% of the total gel slice radioactivity remained in the water layer from [^{3}H]myristate- and [^{3}H]palmitate-labeled cells, respectively. These results indicate that the fatty acyl groups attached to cPLA$_2\gamma$ are ester-linked rather than amide-linked. The radioactivity remaining in the water layer after hydrolysis in 6 M HCl is presumably attributable to radiolabeled amino acids that resulted from metabolic β-oxidation of the radiolabeled fatty acids into acetyl-CoA and then into amino acids in the fibroblasts, but we did not further investigate this water-soluble radiolabeled material.

The material resulting from Dole extraction of the aqueous NaOH-treated sample was treated with pentafluorobenzyl bromide in the presence of the carrier nonradiolabeled fatty acids myristic, palmitic, and oleic acids, and the sample was analyzed by reverse-phase HPLC using ultraviolet absorbance at 254 nm to monitor the carrier fatty acid esters and by scintillation counting to monitor the radiolabel. For [^{3}H]palmitate-labeled cells, two peaks of radioactivity coeluted precisely with the nonradiolabeled oleic acid and palmitic acid ester standards, and no radioactivity eluted with the myristic acid ester standard (Fig. 6B). The HPLC retention times for the myristate and oleate esters are reproducible to within 10 s, a time much shorter than the difference in retention times for the two esters. The radioactivity clearly comigrates with the 18:1 ester without a discernible shoulder at a shorter retention time. These results show that cPLA$_2\gamma$ contains ester-linked oleoyl and palmitoyl groups. The same HPLC pattern was seen for [^{3}H]myristate-labeled cells (data not shown), indicating that the 14 carbon fatty acid was converted to the 16 and 18 carbon fatty acids in fibroblasts and that cPLA$_2\gamma$ is not myristoylated. The formation of the cPLA$_2\gamma$-linked radiolabeled oleoyl group is presumably the result of elongation of the radiolabeled fatty acyl-CoA to stearoyl-CoA followed by the action of stearoyl-CoA desaturase to form oleoyl-CoAs.

Subcellular localization of cPLA$_2\gamma$

The localization of expressed untagged cPLA$_2\gamma$ in fixed IMLF$^{-/-}$, SkMc cells, and COS cells was carried out using a rabbit polyclonal antibody generated against full-length cPLA$_2\gamma$. A comparison of cPLA$_2\gamma$ localization and a variety of organelle markers demonstrated that cPLA$_2\gamma$ localized primarily to mitochondria. The morphology of mitochondria is heterogeneous in cells, but they often appear

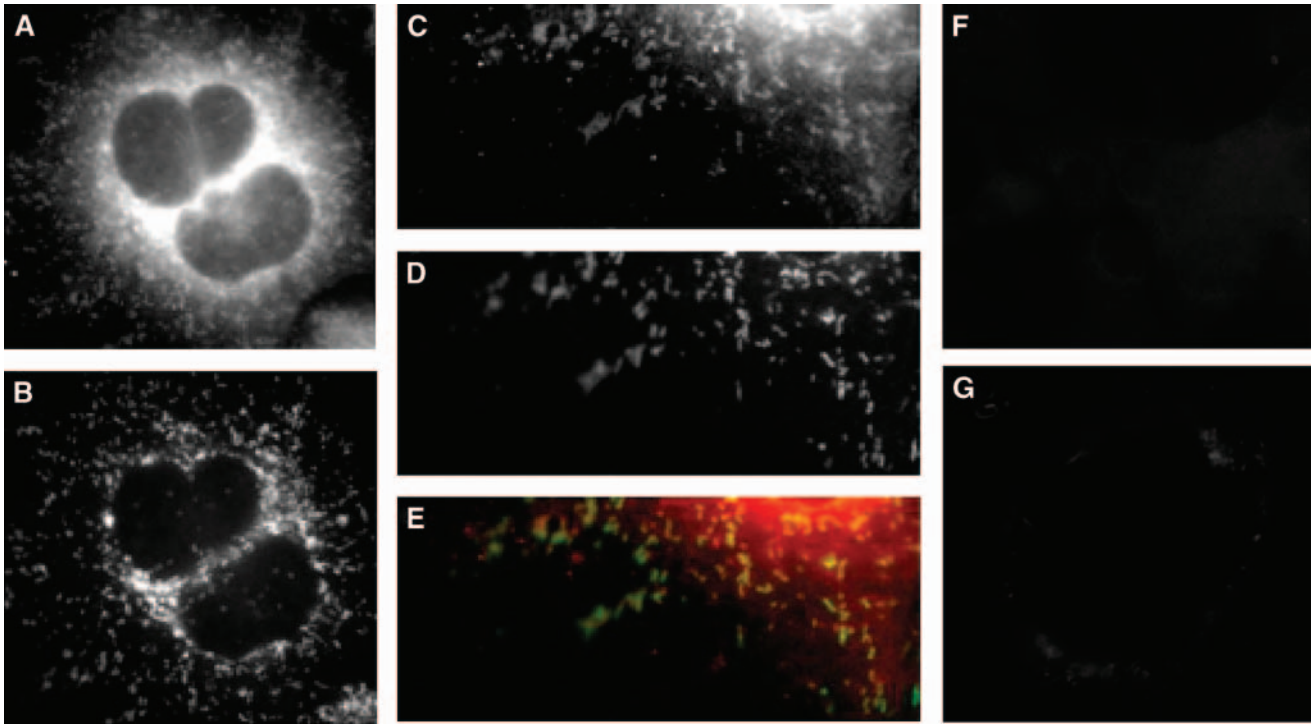

Fig. 7. cPLA$_2$γ localizes to mitochondria in IMLF$^{-/-}$. IMLF$^{-/-}$ were infected with Ad-cPLA$_2$γ, fixed, and probed with polyclonal antiserum to anti-cPLA$_2$γ and monoclonal antibodies to anti-oxidative phosphorylation complex V. Secondary antibodies used were conjugated to Texas Red and AlexaFluor 488, respectively. Immunofluorescence of cPLA$_2$γ (A, C) and of the mitochondrial marker oxidative phosphorylation complex V (B, D) is shown. An overlay of cPLA$_2$γ fluorescence (red) and mitochondrial marker fluorescence (green) is shown (E). IMLF$^{-/-}$ overexpressing cPLA$_2$γ were probed with Texas Red secondary antibody only (F), and probed with anti-oxidative phosphorylation complex V primary monoclonal antibodies and anti-rabbit secondary Texas Red antibodies as controls (G).

as small ovoid structures or branched "threads" (42). Mitochondria often concentrate around the cell nucleus, where they are closely apposed to the endoplasmic reticulum. However, mitochondria can be clearly resolved in the cell periphery, where they are not as closely associated with the endoplasmic reticulum (42).

In IMLF$^{-/-}$, the localization of cPLA$_2$γ was concentrated in the central, thickest region of the cell around the nucleus, where little structural detail could be observed (**Fig. 7**). However, farther out in the cell extensions, cPLA$_2$γ was clearly localized to branched, thread-like structures that stained with antibodies to the mitochondrial marker oxidative phosphorylation complex V, subunit b. The mitochondrial localization of cPLA$_2$γ was also clearly apparent when it was expressed in SkMc cells (**Fig. 8**). cPLA$_2$γ localized on branched, tubular structures that wrapped around the nucleus and extended toward the periphery of the cell, and these structures costained with antibodies to the mitochondrial marker oxidative phosphorylation complex V. Although overexpressed cPLA$_2$γ predominately costained with the mitochondrial markers, there was a small amount of cPLA$_2$γ in these cells that did not colocalize with the endoplasmic reticulum, lysosomes, nucleus, or mitochondria (data not shown). Control experiments with secondary antibody alone (Fig. 7F) as well as each secondary antibody with the opposite primary antibody were negative (Fig. 7G). Additional experiments demonstrated that BMS-214662 had no effect on the localization of cPLA$_2$γ on the mitochondria in SkMc cells (data not shown).

It was suggested recently that N-terminal FLAG-tagged cPLA$_2$γ localizes to the endoplasmic reticulum when expressed in HEK293 cells, based on a cytoplasmic reticular staining pattern, although this was not confirmed with organelle markers (40). In HEK293 cells, FLAG-tagged cPLA$_2$γ was found enriched in the perinuclear region, but no signal was seen on the nuclear envelope, which is an extension of the endoplasmic reticulum (40). In another study, it was reported that cPLA$_2$γ with an N-terminal GFP tag localized at the Golgi, endoplasmic reticulum, and nuclear envelope when expressed in CHO cells but did not colocalize with a lysosomal or mitochondrial marker (26).

The reports suggesting that N-terminal-tagged cPLA$_2$γ primarily localizes to the endoplasmic reticulum and that mutation of the prenylation site affects the localization of FLAG-tagged cPLA$_2$γ are distinct from our results with untagged cPLA$_2$γ (26, 40). Although it is possible that the localization is cell type-dependent, it is also possible that expression of cPLA$_2$γ with an N-terminal tag has an effect on its localization and conformation on the membrane. We have found that N-terminal GFP and 6× histidine (His) tags negatively affect the enzymatic activity of cPLA$_2$γ, resulting in 80% and 60% less activity than in the wild-type enzyme, respectively (25). The N-terminal tags also suppressed the amount of arachidonic acid released by cPLA$_2$γ when expressed in Sf9 cells (**Fig. 9**). We reported

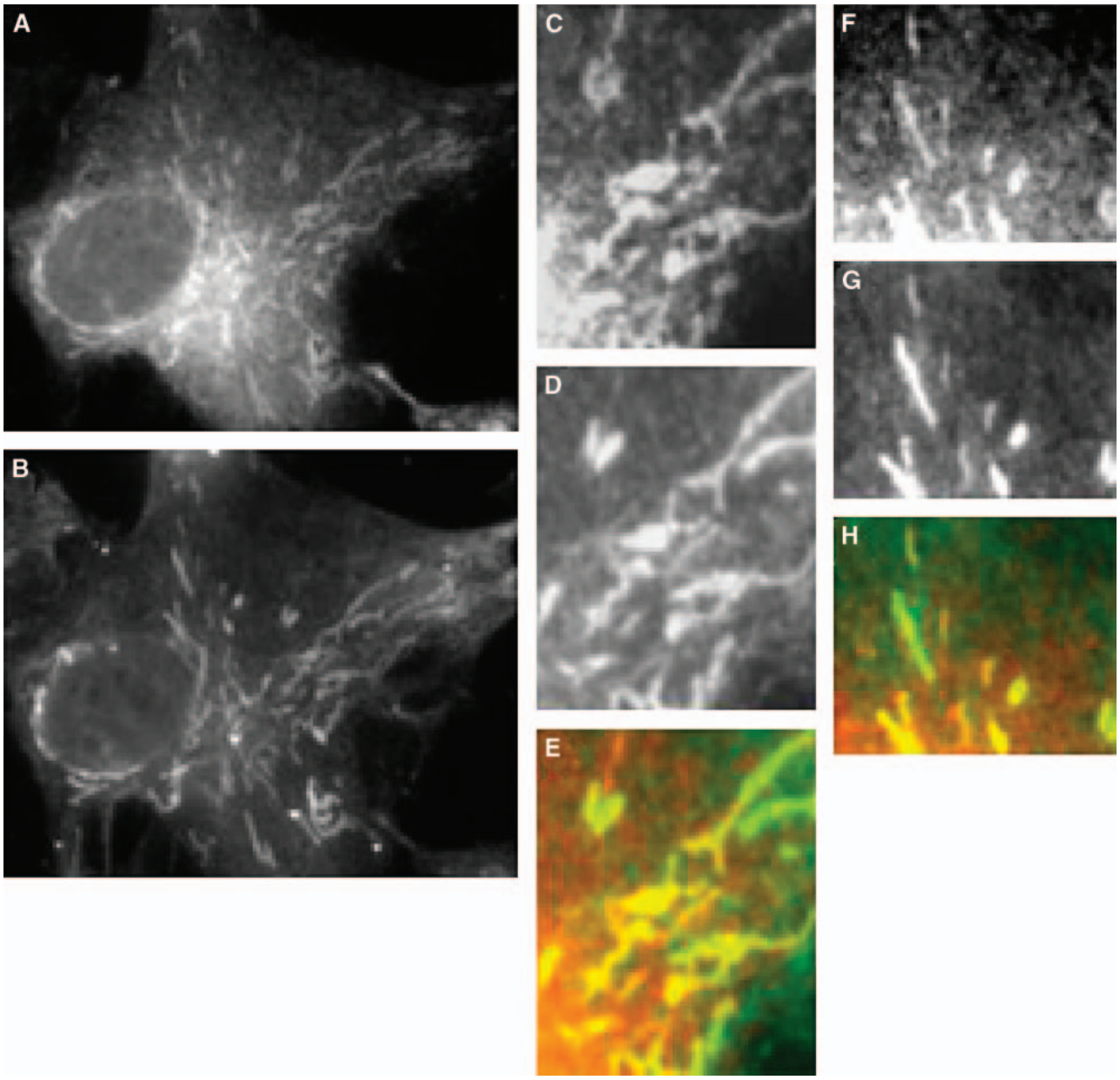

Fig. 8. cPLA$_2\gamma$ localizes to mitochondria in SkMc cells. SkMc cells were infected with Ad-cPLA$_2\gamma$, fixed, and probed with polyclonal antiserum to anti-cPLA$_2\gamma$ and monoclonal antibodies to anti-oxidative phosphorylation complex V. Secondary antibodies used were conjugated to Texas Red and AlexaFluor 488, respectively. Immunofluorescence of cPLA$_2\gamma$ (A, C, F) and of the mitochondrial marker oxidative phosphorylation complex V (B, D, G) is shown. Overlays of cPLA$_2\gamma$ fluorescence (red) and mitochondrial marker fluorescence (green) are shown (E, H).

previously that Sf9 cells can be used as a model to study the function of cPLA$_2\alpha$, which is activated in Sf9 cells by A23187, resulting in the release of arachidonic acid (19, 43). As shown in Fig. 9, A23187 also induced a large increase in arachidonic acid release from Sf9 cells expressing cPLA$_2\gamma$ compared with vector control cells. In contrast to cells expressing untagged cPLA$_2\gamma$, A23187-induced arachidonic acid release from Sf9 cells expressing GFP- or His-tagged cPLA$_2\gamma$ was dramatically reduced to near basal levels, suggesting that the N terminus of the enzyme is critical for the function of cPLA$_2\gamma$. The N-terminal-tagged cPLA$_2\gamma$ enzymes were expressed at similar levels as the wild-type enzyme in Sf9 cells and were constitutively bound to membrane (25). It is important to note that the ability of A23187 to activate cPLA$_2\gamma$ is cell type-specific and is also observed when cPLA$_2\gamma$ is overexpressed in HEK293 cells (40), but A23187 does not stimulate arachidonic acid release from IMLF$^{-/-}$ or SkMc cells overexpressing cPLA$_2\gamma$. The ability of A23187 to activate cPLA$_2\gamma$ is unexpected, because cPLA$_2\gamma$ is calcium-independent; however, an increase in intracellular calcium may trigger unique signals in some cells that play a role in regulating cPLA$_2\gamma$. There is a pronounced lag phase preceding cPLA$_2\gamma$-mediated arachidonic acid release in Sf9 cells treated with A23187, consistent with an indirect mechanism. In contrast, arachidonic acid release from Sf9 cells

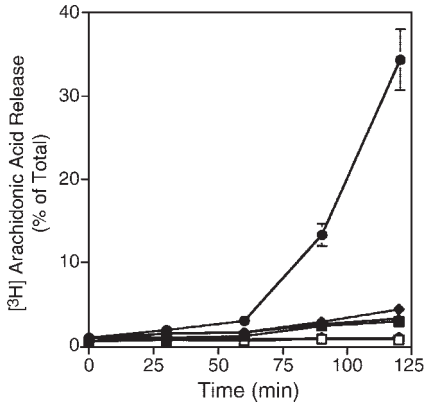

Fig. 9. Effect of N-terminal tags on A23187-stimulated [^{3}H]arachidonic acid release from *Spodoptera frugiperda* (Sf9) cells expressing cPLA$_2\gamma$. [^{3}H]arachidonic acid-labeled Sf9 cells expressing cPLA$_2\gamma$ (circles), 6× histidine-tagged cPLA$_2\gamma$ (diamonds), GFP-cPLA$_2\gamma$ (triangles), or empty vector (squares) were treated with either vehicle (DMSO; open symbols) or 2 μg/ml A23187 (closed symbols) for the times shown. The amount of [^{3}H]arachidonic acid released into the medium is expressed as a percentage of the total incorporated radioactivity. Data shown are averages ± SD of triplicate samples of one experiment that is representative of three independent experiments.

expressing cPLA$_2\alpha$ occurs rapidly in response to A23187, as reported previously, as a result of the direct effect of Ca^{2+} binding to the C2 domain of cPLA$_2\alpha$ and inducing translocation to the membrane (19, 43). We have also observed similar differences in the time course of serum-induced arachidonic acid release from IMLF$^{-/-}$ expressing cPLA$_2\gamma$ and cPLA$_2\alpha$ (25).

DISCUSSION

The results of this study demonstrate that cPLA$_2\gamma$ is farnesylated in mammalian cells and document that prenylation plays a role in cPLA$_2\gamma$-induced fatty acid hydrolysis. The C-terminal residue of cPLA$_2\gamma$ is alanine, and it may be noted that yeast α-factor also has a CaaX box with an X residue of alanine and is farnesylated. It is currently thought that the most preferred substrates for protein geranylgeranyltransferase type I have a CaaX box in which X is leucine or phenylalanine (28). Our studies with cPLA$_2\gamma$ show that not all proteins with a CCXX sequence are doubly geranylgeranylated. Rab proteins have been shown to contain sequences in addition to the double cysteine motif that are recognized by the Rab escort protein that delivers the Rab protein to protein geranylgeranyltransferase type II (44).

The mechanism involved in regulating cPLA$_2\gamma$ function by farnesylation is not known, but our results suggest that it alone is not responsible for membrane binding. For membrane targeting of other farnesylated proteins such as Ras, the farnesylated C terminus is not sufficient but requires either a polybasic domain or protein fatty acylation (45). In addition to membrane anchoring, prenylation can play a role in the heterodimeric protein interaction that is proposed to involve a two-site recognition (46). cPLA$_2\gamma$ also has a cluster of basic residues adjacent to a hydrophobic region in the C terminus that may be significant in its association with the membrane (30). Because cPLA$_2\gamma$ mutated at the prenylation site does not separate to the soluble fraction in the presence of 1.0 M NaCl, electrostatic interactions and prenylation alone are unlikely to determine the membrane binding of cPLA$_2\gamma$. To investigate the role that the hydrophobic and basic regions in the cPLA$_2\gamma$ C terminus may play in membrane binding more thoroughly, a truncated cPLA$_2\gamma$, missing these regions, was created. However, our results indicate no change in membrane association of cPLA$_2\gamma$ attributable to this mutation, suggesting that these regions do not play a predominant role in membrane association. In addition to experiments to determine the possible mechanism of farnesylation, fatty acid labeling experiments were conducted using cells expressing wild-type cPLA$_2\gamma$ and the C538S mutant. Farnesylation could be required for the fatty acylation of cPLA$_2\gamma$. However, our data indicate that this is not the case for cPLA$_2\gamma$, because the fatty acid labeling is not significantly changed when the prenylation site is mutated (data not shown).

cPLA$_2\gamma$ contains a putative N-myristoylation site; however, our results demonstrate that cPLA$_2\gamma$ is acylated with palmitic and oleic acids, but we saw no evidence that myristoylation of the enzyme occurs. Consistent with this observation, we found that cPLA$_2\gamma$ mutated at both the N-terminal glycine (to block possible myristoylation) and the prenylation site remains bound to the membrane (data not shown). Although cPLA$_2\gamma$ is radiolabeled with [^{3}H]myristic acid, it is first metabolized into [^{3}H]palmitic and [^{3}H]oleic acids, which subsequently associate with cPLA$_2\gamma$. Thus, although our data show that N-terminal tags on cPLA$_2\gamma$ negatively affect function, this is not attributable to blocking myristoylation but may have an affect on enzyme conformation, acylation, or membrane trafficking. Although these results indicate that cPLA$_2\gamma$ is fatty acylated, the locations of the oleic and palmitic acyl groups on the protein chain remain to be determined. It is possible that both types of fatty acyl groups could be linked to the same residue or that the enzyme could be acylated on multiple residues. Investigation of mutations of the individual cysteines is under way. However, the more rare palmitoylation of serine or threonine residues via oxyester bonds can also occur and must be considered.

The observation that cPLA$_2\gamma$ primarily associates with mitochondria suggests that it may play a role in the function of this organelle. Although cPLA$_2\gamma$ message is abundant in human SkMc, to date, primarily immortalized cells have been used to study cPLA$_2\gamma$ (21, 23, 25, 26, 40). By RT-PCR, we have confirmed that cPLA$_2\gamma$ message is produced in both myotubes and myoblasts of SkMc cells (data not shown). However, despite the presence of message, only very low levels of endogenous cPLA$_2\gamma$ protein were detectable in SkMc cells, making the direct study of endogenous cPLA$_2\gamma$ difficult. The regulation of membrane binding and localization of cPLA$_2\gamma$ to mitochondria are very different from the known properties of cPLA$_2\alpha$, which

has not been shown to associate with mitochondria. Recently, an increase in the group IVC $cPLA_2$ in apoptotic macrophage cells was observed (47). This observation suggests a potential role in the mitochondrial induction of apoptosis for $cPLA_2\gamma$. Both calcium-dependent and -independent PLA_2 activities have been found associated with isolated mitochondria, including the group VI calcium-independent PLA_2 and the group IIA $sPLA_2$ (48–51). The presence of diverse PLA_2 enzymes in mitochondria suggests that there are multiple, independently regulated pathways in this organelle for the hydrolysis of membrane phospholipid.

This work was supported by National Institutes of Health Grants HL-34303 and HL-61378 (C.C.L.), HL-50040 (M.H.G.), and by an Individual National Research Service Award (HL-77064 to D.E.T.).

REFERENCES

1. Six, D. A., and E. A. Dennis. 2000. The expanding superfamily of phospholipase A_2 enzymes: classification and characterization. *Biochim. Biophys. Acta.* **1488:** 1–19.
2. Murakami, M., and I. Kudo. 2001. Diversity and regulatory functions of mammalian secretory phospholipase A_2s. *Adv. Immunol.* **77:** 163–194.
3. Valentin, E., and G. Lambeau. 2000. Increasing molecular diversity of secreted phospholipases A_2 and their receptors and binding proteins. *Biochim. Biophys. Acta.* **1488:** 59–70.
4. Winstead, M. V., J. Balsinde, and E. A. Dennis. 2000. Calcium-independent phospholipase A_2: structure and function. *Biochim. Biophys. Acta.* **1488:** 28–39.
5. Sharp, J. C., R. T. Pickard, X. G. Chiou, J. V. Manetta, S. Kovacevic, J. R. Miller, A. D. Varshavsky, E. F. Roberts, B. A. Strifler, D. N. Brems, et al. 1994. Serine 228 is essential for catalytic activities of 85-kDa cytosolic phospholipase A_2. *J. Biol. Chem.* **269:** 23250–23254.
6. Clark, J. D., A. R. Schievella, E. A. Nalefski, and L-L. Lin. 1995. Cytosolic phospholipase A_2. *J. Lipid Mediat. Cell Signal.* **12:** 83–117.
7. Tang, J., R. W. Kriz, N. Wolfman, M. Shaffer, J. Seehra, and S. S. Jones. 1997. A novel cytosolic calcium-independent phospholipase A_2 contains eight ankyrin motifs. *J. Biol. Chem.* **272:** 8567–8575.
8. Leslie, C. C. 1997. Properties and regulation of cytosolic phospholipase A_2. *J. Biol. Chem.* **272:** 16709–16712.
9. Leslie, C. C. 2004. Regulation of arachidonic acid availability for eicosanoid production. *Biochem. Cell Biol.* **82:** 1–17.
10. Leslie, C. C. 2004. Regulation of the specific release of arachidonic acid by cytosolic phospholipase A_2. *Prostaglandins Leukot. Essent. Fatty Acids.* **70:** 373–376.
11. Funk, C. D. 2001. Prostaglandins and leukotrienes: advances in eicosanoid biology. *Science.* **294:** 1871–1875.
12. Lin, L-L., M. Wartmann, A. Y. Lin, J. L. Knopf, A. Seth, and R. J. Davis. 1993. $cPLA_2$ is phosphorylated and activated by MAP kinase. *Cell.* **72:** 269–278.
13. Hefner, Y., A. G. Borsch-Haubold, M. Murakami, J. I. Wilde, S. Pasquet, D. Schieltz, F. Ghomashchi, J. R. Yates 3rd, C. G. Armstrong, A. Paterson, et al. 2000. Serine 727 phosphorylation and activation of cytosolic phospholipase A_2 by MNK1-related protein kinases. *J. Biol. Chem.* **275:** 37542–37551.
14. Muthalif, M. M., Y. Hefner, S. Canaan, J. Harper, H. Zhou, J-H. Parmentier, R. Aebersold, M. H. Gelb, and K. U. Malik. 2001. Functional interaction of calcium-/calmodulin-dependent protein kinase II and cytosolic phospholipase A_2. *J. Biol. Chem.* **276:** 39653–39660.
15. Channon, J., and C. C. Leslie. 1990. A calcium-dependent mechanism for associating a soluble arachidonoyl-hydrolyzing phospholipase A_2 with membrane in the macrophage cell line, RAW 264.7. *J. Biol. Chem.* **265:** 5409–5413.
16. Clark, J. D., L-L. Lin, R. W. Kriz, C. S. Ramesha, L. A. Sultzman, A. Y. Lin, N. Milona, and J. L. Knopf. 1991. A novel arachidonic acid-selective cytosolic PLA_2 contains a Ca^{2+}-dependent translocation domain with homology to PKC and GAP. *Cell.* **65:** 1043–1051.
17. Glover, S., M. S. de Carvalho, T. Bayburt, M. Jonas, E. Chi, C. C. Leslie, and M. H. Gelb. 1995. Translocation of the 85-kDa phospholipase A_2 from cytosol to the nuclear envelope in rat basophilic leukemia cells stimulated with calcium ionophore or IgE/antigen. *J. Biol. Chem.* **270:** 15359–15367.
18. Nalefski, E. A., L. A. Sultzman, D. M. Martin, R. W. Kriz, P. S. Towler, J. L. Knopf, and J. D. Clark. 1994. Delineation of two functionally distinct domains of cytosolic phospholipase A_2, a regulatory Ca^{2+}-dependent lipid-binding domain and a Ca^{2+}-independent catalytic domain. *J. Biol. Chem.* **269:** 18239–18249.
19. Gijón, M. A., D. M. Spencer, A. L. Kaiser, and C. C. Leslie. 1999. Role of phosphorylation sites and the C2 domain in regulation of cytosolic phospholipase A_2. *J. Cell Biol.* **145:** 1219–1232.
20. Evans, J. H., D. M. Spencer, A. Zweifach, and C. C. Leslie. 2001. Intracellular calcium signals regulating cytosolic phospholipase A_2 translocation to internal membranes. *J. Biol. Chem.* **276:** 30150–30160.
21. Underwood, K. W., C. Song, R. W. Kriz, X. J. Chang, J. L. Knopf, and L-L. Lin. 1998. A novel calcium-independent phospholipase A_2, $cPLA_2$-γ, that is prenylated and contains homology to $cPLA_2$. *J. Biol. Chem.* **273:** 21926–21932.
22. Pickard, R. T., B. A. Strifler, R. M. Kramer, and J. D. Sharp. 1999. Molecular cloning of two new human paralogs of 85-kDa cytosolic phospholipase A_2. *J. Biol. Chem.* **274:** 8823–8831.
23. Song, C., X. J. Chang, K. M. Bean, M. S. Proia, J. L. Knopf, and R. W. Kriz. 1999. Molecular characterization of cytosolic phospholipase A_2-β. *J. Biol. Chem.* **274:** 17063–17067.
24. Clissold, P. M., and C. P. Ponting. 2001. JmjC: cupin metalloenzyme-like domains in jumonji, hairless and phospholipase A2beta. *Trends Biochem. Sci.* **26:** 7–9.
25. Stewart, A., M. Ghosh, D. M. Spencer, and C. C. Leslie. 2002. Enzymatic properties of human cytosolic phospholipase $A_2\gamma$. *J. Biol. Chem.* **277:** 29526–29536.
26. Asai, K., T. Hirabayashi, T. Houjou, N. Uozumi, R. Taguchi, and T. Shimizu. 2003. Human group IVC phospholipase A_2 ($cPLA_2\gamma$). Roles in the membrane remodeling and activation induced by oxidative stress. *J. Biol. Chem.* **278:** 8809–8814.
27. Leslie, C. C. 1991. Kinetic properties of a high molecular mass arachidonoyl-hydrolyzing phospholipase A_2 that exhibits lysophospholipase activity. *J. Biol. Chem.* **266:** 11366–11371.
28. Yokoyama, K., G. W. Goodwin, F. Ghomashchi, J. Glomset, and M. H. Gelb. 1992. Protein prenyltransferases. *Biochem. Soc. Trans.* **20:** 489–494.
29. Casey, P. J., and M. C. Seabra. 1996. Protein prenyltransferases. *J. Biol. Chem.* **271:** 5289–5292.
30. Jenkins, C. M., X. Han, J. Yang, D. J. Mancuseo, H. F. Sims, A. J. Muslin, and R. W. Gross. 2003. Purification of recombinant human $cPLA_2\gamma$ and identification of C-terminal farnesylation, proteolytic processing, and carboxymethylation by MALDI-TOF-TOF analysis. *Biochemistry.* **42:** 11798–11807.
31. Farnsworth, C. C., M. C. Seabra, L. H. Ericsson, M. H. Gelb, and J. A. Glomset. 1994. Rab geranylgeranyl transferase catalyzes the geranylgeranylation of adjacent cysteines in the small GTPases Rab1A, Rab3A, and Rab5A. *Proc. Natl. Acad. Sci. USA.* **91:** 11963–11967.
32. Smotrys, J. E., and M. E. Linder. 2004. Palmitoylation of intracellular signaling proteins: regulation and function. *Annu. Rev. Biochem.* **73:** 559–587.
33. Resh, M. D. 2004. Membrane targeting of lipid modified signal transduction proteins. *Subcell. Biochem.* **37:** 217–232.
34. Corvi, M. M., C. L. Soltys, and L. G. Berthiaume. 2001. Regulation of mitochondrial carbamoyl-phosphate synthetase 1 activity by active site fatty acylation. *J. Biol. Chem.* **276:** 45704–45712.
35. Farazi, T. A., G. Waksman, and J. I. Gordon. 2001. The biology and enzymology of protein N-myristoylation. *J. Biol. Chem.* **276:** 39501–39504.
36. Bijlmakers, M., and M. Marsh. 2003. The on-off story of protein palmitoylation. *Trends Cell Biol.* **13:** 32–42.
37. Hunt, J. T., C. Z. Ding, R. Batorsky, M. Bednarz, R. Bhide, Y. Cho, S. Chong, S. Chao, J. Gull-Brown, P. Guo, et al. 2000. Discovery of (R)-7-cyano-2,3,4,5-tetrahydro-1-(1H-imidazol-4-ylmethyl)-3-(phenylmethyl)-4-(2-thienylsulfonyl)-1H-1,4-benzodiazepine (BMS-214662), a farnesyltransferase inhibitor with potent preclinical antitumor activity. *J. Med. Chem.* **43:** 3587–3595.
38. Ghosh, M., A. Stewart, D. E. Tucker, J. V. Bonventre, R. C. Murphy, and C. C. Leslie. 2004. Role of cytosolic phospholipase A_2 in pros-

taglandin E_2 production by lung fibroblasts. *Am. J. Respir. Cell Mol. Biol.* **30:** 91–100.
39. Whitten, M. E., K. Yokoyama, D. Schieltz, F. Ghomashchi, D. Lam, J. R. Yates, K. Palczewski, and M. H. Gelb. 2000. Structural analysis of protein prenyl groups and associated C-terminal modifications. *Methods Enzymol.* **316:** 436–451.
40. Murakami, M., S. Masuda, and I. Kudo. 2003. Arachidonate release and prostaglandin production by group IVC phospholipase A_2 (cytosolic phospholipase $A_2\gamma$). *Biochem. J.* **372:** 695–702.
41. Bernstein, L. S., M. E. Linder, and J. R. Helper. 2004. Analysis of RGS protein palmitoylation. *Methods Mol. Biol.* **237:** 195–204.
42. Collins, T. J., M. J. Berridge, P. Lipp, and M. D. Bootman. 2002. Mitochondria are morphologically and functionally heterogeneous within cells. *EMBO J.* **21:** 1616–1627.
43. de Carvalho, M. G. S., A. L. McCormack, E. Olson, F. Ghomashchi, M. H. Gelb, J. R. Yates III, and C. C. Leslie. 1996. Identification of phosphorylation sites of human 85-kDa cytosolic phospholipase A_2 expressed in insect cells and present in human monocytes. *J. Biol. Chem.* **271:** 6987–6997.
44. Pereira-Leal, J. B., M. Strom, R. F. Godfrey, and M. C. Seabra. 2003. Structural determinants of Rab and Rab escort protein interaction: Rab family motifs define a conserved binding surface. *Biochem. Biophys. Res. Commun.* **301:** 92–97.
45. Hancock, J. F., H. F. Paterson, and C. J. Marshall. 1990. A polybasic domain or palmitoylation is required in addition to the CAAX motif to localize p21ras to the plasma membrane. *Cell.* **63:** 133–139.
46. Sinensky, M. 2000. Functional aspects of polyisoprenoid protein substituents: role in protein-protein interaction and trafficking. *Biochim. Biophys. Acta.* **1529:** 203–209.
47. Duan, L., H. Gan, J. Arm, and J. Remold. 2001. Cytosolic phospholipase A_2 participates with TNF-α in the induction of apoptosis of human macrophages infected with *Mycobacterium tuberculosis* H37Ra. *J. Immunol.* **166:** 7469–7476.
48. Williams, S. D., and R. A. Gottlieb. 2002. Inhibition of mitochondrial calcium-independent phospholipase A_2 ($iPLA_2$) attenuates mitochondrial phospholipid loss and is cardioprotective. *Biochem. J.* **362:** 23–32.
49. Broekemeier, K. M., J. R. Iben, E. G. LeVan, E. D. Crouser, and D. R. Pfeiffer. 2002. Pore formation and uncoupling initiate a Ca^{2+}-independent degradation of mitochondrial phospholipids. *Biochemistry.* **41:** 7771–7780.
50. Guidarelli, A., and O. Cantoni. 2002. Pivotal role of superoxides generated in the mitochondrial respiratory chain in peroxynitrite-dependent activation of phospholipase A_2. *Biochem. J.* **366:** 307–314.
51. Aarsman, A. J., J. G. N. de Jong, E. Arnoldussen, F. W. Neys, P. D. van Wassenaar, and H. Van den Bosch. 1989. Immunoaffinity purification, partial sequence, and subcellular localization of rat liver phospholipase A_2. *J. Biol. Chem.* **264:** 10008–10014.